Carbohydrate Polymer Technologies and Applications 8 (2024) 100566

Contents lists available at ScienceDirect

Carbohydrate Polymer Technologies and Applications

journal homepage: www.sciencedirect.com/journal/carbohydrate-polymer-technologies-and-applications

Xyloglucan, alginate and k-carrageenan hydrogels on spheroids of adipose stem cells survival; preparation, mechanical characterization, morphological analysis and injectability

Emanuela Muscolino [a,b], Anna Barbara Di Stefano [c,*], Francesca Toia [c,d], Daniela Giacomazza [b], Francesco Moschella [c], Adriana Cordova [c,d], Clelia Dispenza [a]

[a] Dipartimento di Ingegneria, Università degli Studi di Palermo, Viale delle Scienze 6, 90128 Palermo, Italy
[b] Istituto di BioFisica, Consiglio Nazionale delle Ricerche, Via U. La Malfa 153, 90146 Palermo, Italy
[c] BIOPLAST-Laboratory of BIOlogy and Regenerative Medicine-PLASTic Surgery, Dipartimento di Medicina di Precisione in Area Medica, Chirurgica e Critica, Università degli Studi di Palermo, via del Vespro 129, 90127, Palermo, Italy
[d] Unità di Chirurgia Plastica e Ricostruttiva, Medicina di Precisione in Area Medica, Chirurgica e Critica, Università degli Studi di Palermo, via del Vespro 129, 90127, Palermo, Italy

ARTICLE INFO

Keywords:
Mesenchymal stem cells (MSCs)
Spheroids of adipose stem cell (SASCs)
Different chemical structure hydrogels
Polysaccharides
Biomechanical cues
Degalactosylated xyloglucan

ABSTRACT

The therapeutic capabilities of autologous stem cells can be fully exploited if their survival after implantation is improved.

For the first time, we compared three hydrogels, with different chemical structure, morphology, and viscoelastic properties, where the same differentiation factors were immobilized and spheroids from adipose stem cells (SASCs) were incorporated. The aim is to understand if hydrogel characteristics could influence the viability of the embedded stem cells. Specifically, hydrogels of partially degalactosylated xyloglucan (dXG), sodium alginate (Alg) and k-carrageenan (kC) were produced. The structure of the networks was probed by swelling/erosion measurements, rheological and morphological analysis. Cell viability was measured after 7 and 21 days. When SASCs were incubated under stemness conditions, dXG and kC hydrogels provide the optimal environment for cell viability. When incubated in the chondrogenic or osteogenic medium, a clear correlation was found between the storage and loss moduli and cell viability. Hydrogels with the lowest shear stiffness promote stem-cell differentiation and proliferation. The systems, particularly dXG, seem more similar to natural ECM and able to recreate niches, that colonized with stem cells could represent a real support in regenerative therapies. The injectability of formulations was evaluated to determine if they could be used for minimally invasive regenerative medicine interventions.

1. Introduction

The possibility of using autologous stem cells for the regeneration and repair of articular defects opens up exciting prospects for the treatment of degenerative diseases, such as osteoarthritis, affecting articular cartilage. A first challenge is to localize and immobilize stem cells at the appropriate site and to ensure that they have the most suitable conditions for survival, differentiation, and proliferation. Stem cells-laden biodegradable and injectable hydrogels can ensure cell localization, promote cell engraftment, and direct cell life cycle.

Stem cells live in a distinctive microenvironment, called *niche*, which consists of cellular and noncellular constituents that offer mechanical support to cells but also biophysical and biochemical cues that influence cell behavior. The niche is formed by the extra cellular matrix (ECM), a mixture of long chain polysaccharides, fibrous proteins and sugars, and cellular secreted factors, such as growth factors, immunological factors and metabolic signals (de Groot et al., 2020; Shrestha & Yoo, 2019). ECMs have been recreated and artificially engineered to study the role of the stem cell niche on stem cell fate and to be able to offer cell regeneration solutions to a variety of medical conditions (de Groot et al., 2020; Li et al., 2006).

Polysaccharide-based hydrogels are utilized across various fields for their structural properties and compatibility with diverse environments. Their biocompatibility makes them suitable for use with living tissues

* Corresponding author.
E-mail address: annabarbara.distefano@unipa.it (A.B. Di Stefano).

https://doi.org/10.1016/j.carpta.2024.100566

Available online 13 September 2024

without causing toxic or immune responses. Hydrogel scaffolds are ideal for cartilage regeneration, mimicking the aqueous and nanofibrous nature of cartilage ECM. Their 3D network allows significant swelling, aiding in the encapsulation and diffusion of cells, nutrients, and gases (Bahram et al., 2016; Chen et al., 2004; Nayyer et al., 2012). These materials can be engineered to optimize cell adhesion and preserve bioactive molecules, promoting cell growth and differentiation, but also to encapsulate and inject organelles, like mitochondria (Picone et al., 2024).

Hydrogels are often considered good ECM mimics, for their structural and/or morphological similarities with natural ECMs, their high hydration levels and interconnected pore architecture (Chen et al., 2004; Nayyer et al., 2012; Stoddart et al., 2009; Zhu & Marchant, 2011). Hydrogels can act as artificial ECMs for MSCs, either derived from decellularized ECMs or fabricated from synthetic and natural polymers (Fitzpatrick & McDevitt, 2015; Hoshiba et al., 2010). Injectable hydrogels ensure cell retention and optimal microenvironment reconstruction with minimal invasiveness, suitable for complex lesions (Aguado et al., 2012; Liang et al., 2013). Engineering these niches using biocompatible, plant-derived polymers that form physical gels under physiological conditions can reduce immunogenic responses and simplify scale-up and regulatory processes (Toia et al., 2020). Although stem cell differentiation in artificial ECM has conventionally been stimulated and controlled with cocktails of different growth factors, it has also recently been gradually linked to mechanobiological concepts, and the physical forces that are established between cells and matrix (Reilly & Engler, 2010).

Understanding the key parameters for securing stem cell performance is crucial but complex. Factors include the stem cell source, isolation and storage procedures, formulation composition, biochemical cues, gelation mechanism and kinetics, hydrogel viscoelastic properties, morphological features, and how these properties change over time and in response to the environment. Cell response to matrix stiffness varies with cell and ligand types and can alter cell matrix deposition or activate matrix remodeling, affecting stiffness (Janmey et al., 2020). In most studies, biomechanical stimulation has been provided by controlling substrate stiffness through matrix chemistry and cross-linking density of covalent networks. Often the change in stiffness is accompanied by changes in porosity and/or topology, and it is very difficult to decouple their effects. These artificial niches also lack an important feature of natural niches: dynamics and viscoplasticity (Petzold & Gentleman, 2021).

Natural ECM networks are mainly noncovalent, forming cross-linking points through multiple weak interactions, allowing stress relaxation, material flow, and reformation. Stress relaxation has been shown to favor cell migration (Adebowale et al., 2021; Wu et al., 2023). The two components of the complex shear modulus, the storage modulus related to Young's modulus (which measures stiffness), and the loss modulus (which measures energy dissipation) provide a more complete description of the biomechanical microenvironment.

This study compares different physical hydrogels as artificial niches for spheroids of human adipose stem cells from lipoaspirate of volunteer donors. The cells were isolated from the tissue, purified, and cultured under serum-free and low-adhesion conditions. These spheroids have been fully characterized and their important regenerative potential, capacity to differentiate in different cellular lineages depending on the stimulation and to actively participate in bone tissue regeneration in a small animal model were demonstrated (Di Stefano et al., 2016, 2021).

The hydrogels used are based on three polysaccharides: a partially degalactosylated xyloglucan (dXG), produced in house from tamarind seed xyloglucan (XG), sodium alginate (Alg) and k-carrageenan (kC). All these polysaccharides can form hydrogels with no recourse to chemical crosslinking agents and in mild conditions. They are all potentially suited for use as gelling components in degradable injectable formulations. XG is composed of a β-(1, 4)-D-glucan backbone chain that is partially substituted by α-(1, 6)-D-xylose. Some of the xylose residues are substituted by β-(1, 2)-D-galactoxylose (D. Chen et al., 2012). The interest on this polymer derives from the evidence that galactose-carrying polymers can guide adipocyte adhesion through receptor-mediated interactions (Cho et al., 2006; Yin, 2003) and favor cell attachment in keratinocytes cells that can recognize the galactose residues (Klíma et al., 2009; Panjwani, 2014). After a simple enzymatic modification to remove between 35 % and 50 % of the galactose residues, dXG can undergo gelation upon a temperature increase from room temperature (25 °C) to body temperature (37 °C) (Brun-Graeppi et al., 2010; Chen et al., 2012; Shirakawa et al., 1998), that is also a very interesting feature for the envisaged application. Its molecular weight can be modified by high-energy irradiation to alter gelation kinetics and gel microstructure (Muscolino et al., 2023; Todaro et al., 2016). Moreover, we have demonstrated that 1 %w dXG hydrogels incubated in SCM can preserve SASC viability and stemness (Toia et al., 2020). When formulated and incubated with CDM or ODM, they differentiate in chondroblasts and in osteocytes, respectively, and proliferate within the scaffold (Muscolino et al., 2021).

Alginate is an anionic polymer, made of α-L-guluronic and β-D-mannuric acid residues. In dilute solution, the chains form dimers with Ca^{2+}, which then aggregate to gelation (Rinaudo, 1993). Mesenchymal stem cell (MSC) spheroids have been embedded within alginate hydrogels (Ho et al., 2016). Data support that when MSCs are deployed as spheroids in alginate gels, they exhibit increased cell survival. kC is a linear galactan with an ester sulfate content of 15 %–40 % (w/w), containing alternating (1, 3)-α-D and (1, 4)-β-D-galactopyranosyl linkages (El-Fawal et al., 2017; Necas & Bartosikova, 2013; Zhang et al., 2015). Owing to its backbone conformation, this polysaccharide looks like the innately occurring glycosaminoglycans which are the central constituents of connective tissues (Zhang et al., 2015). kC is water-soluble at temperature above 60 °C and can set into stable gels with decreasing temperature (Mangione et al., 2003). kC in blend with PVA has been used to produce scaffolds with enhanced cell adhesion (Muscolino, Costa, et al., 2022) and evaluated as temperature-responsive bio-ink for 3D printing of scaffolds to be seeded or co-printed with SASCs. SASCs survival after co-printing with kC/PVA was indeed very good. After 21 days incubation with CDM, the stem cells were differentiated in chondrocytes (Muscolino, Di Stefano, et al., 2022).

In this study, we assessed and compared the properties of these three physical hydrogels, each differing in chemical structure, morphology, and viscoelastic characteristics, in which the same differentiation factors were immobilized and spheroids of adipose stem cells (SASCs) were incorporated. The objective was to determine how these various hydrogel properties might affect the viability of the embedded stem cells.

2. Experimentals

2.1. Materials

Tamarind seeds xyloglucan was purchased from Megazyme International (Ireland). Sugar composition of the tamarind seed xyloglucan is xylose 34 %w; glucose 45 %w; galactose 17 %w; arabinose and other sugars 4 %w, as provided by Megazyme International. β-Galactosidase from Aspergillus oryzae (11.8 U/mg) was purchased from Sigma Chemicals (USA). Tamarind seeds xyloglucan was degalactosylated (dXG) according to an established protocol, to obtain a degalactosylated degree of ca. 45 % (Brun-Graeppi et al., 2010; Shirakawa et al., 1998). k-Carrageenan (kC) was provided from Gelcarin ME 8625 FMC Biopolymer. Sodium Alginate (Alg) ($NaC_6H_7O_6$) and calcium chloride ($CaCl_2$) were purchased from Sigma-Aldrich. Sodium Phosphate Dibasic (SFD), Potassium Phosphate Monobasic (PFM) and Sodium Chloride (NaCl) were purchased from Sigma-Aldrich and used to prepare a phosphate-buffered saline (PBS) solution (SFD 0.111 %w, PFM 0.032 % w and NaCl 0.85 %w). Sodium azide (NaN_3) was purchased from

Sigma-Aldrich. Stem cell medium (SCM) was homemade and composed principally by DMEM/F12 salts with added basic fibroblast growth factor (bFGF, 10 ng/ml) and epidermal growth factor (EGF, 20 ng/ml) purchased from Sigma-Aldrich. StemPro® Chondrogenesis Differentiation kit (CDM) and StemPro® Osteogenesis Differentiation Kit (ODM) were purchased from Thermo Fisher Scientific. MTS analysis (3-(4, 5-dimethylthiazol-2-yl)-5-(3-carboxymethoxyphenyl)-2-(4-sulfophenyl)-2H-tetrazolium) was puchased from Promega. Rabbit legs were purchased from the food market

The molecular weight distribution of the three polymers was determined by gel permeation chromatography, calibrated with Pullulans standards, performed with the Agilent 1260 Infinity HPLC, coupled to a refraction index (RI) detector, using two Shodex SB HQ columns (804 and 806) connected in series on sample prepared as 0.1 %w aqueous dispersions, filtered through 0.80-micron membrane syringe filters prior to analysis to remove contaminants, and eluted with 0.02 %w NaN_3 solution at 0.6 ml/min. When the chromatograms are plotted against the molecular weight (Mw) the conversion from elution volume to Mw is performed using the following empirical equation, derived from the analysis of standard polymers (pullulans) with defined molecular weights (i.e., the calibration curve):

$$Log\ Mw[\mathrm{Da}] = 12.75 - 0.49\ V\ [\mathrm{ml}]$$

where V is the elution volume calculated considering the elution flow of 0.6 ml/min.

All molecular masses reported in this work are based on pullulan standards and are not absolute. The chromatograms are shown in **Figure S1** of Supporting information. All the three polysaccharides are relatively polydisperse. The weight average molecular weights are 300 kDa, 1.3 MDa and 2.3 MDa for Alg, dXG and kC, respectively.

2.2. Spheroids of adipose stem cells (SASCs)

Adipose tissue was collected from healthy individuals (12 females and 5 males, mean BMI of 28.5 and mean age of 51.0 years), following approval of an informed consensus. Lipoaspirate samples were harvested from different body areas such as abdomen, breast, flanks, trochanteric region. After mechanic (shake 30 min at 37 °C) and enzymatic (collagenase 150 mg/ml, Gibco, Carlsbad, CA) digestion, the samples were centrifuged at 1200 rpm for 5 min and the stromal vascular fraction (SVF) was resuspended in specific medium. For 3D cultures, the SASCs were plated in stem cell medium (SCM) composed principally by DMEM/F12 salts with added basic fibroblast growth factor (bFGF, 10 ng/ml; Sigma, St. Louis, MO) and epidermal growth factor (EGF, 20 ng/ml, Sigma). SASCs were grown as fluctuating spheroids in an ultra-low attachment culture flask (Corning, NY) (Di Stefano et al., 2016). All systems were added of a small volume of antibiotic-antimycotic solution (1X, Gibco) to prevent bacterial and fungal contamination. Culture flasks were placed at 37 °C in a humidified 5 % CO_2 incubator. The media of SASCs yields obtained were one million for ten ml of adipose tissue.

After spheroids isolation, they were plated in adherent conditions for chondroblastic or osteoblastic differentiation according to StemPro® Chondrogenesis Differentiation kit (CDM) or StemPro® Osteogenesis Differentiation Kit (ODM) protocols (Invitrogen) and maintained at 37 °C in a humidified 5 % CO_2 incubator for 7 and 21 days.

2.3. Hydrogel preparation

dXG powder was weighted and added to 0.22 μm pre-filtered water, to prepare solutions at 2 %w and 5 %w concentration, and stirred for about 2 h at 5 °C until a homogenous dispersion was obtained. Afterwards, the dispersions were sterilized by autoclaving at 121 °C for 20 min. dXG systems cannot be strictly considered solutions, i.e., completely devoid of chain aggregates. This is due to the presence of galactose-bare sequences in the chains that cause side-by-side association of few segments of different chains forming condensed domains (Todaro et al., 2015). The dispersions were stored at 4 °C.

Table 1
Final composition of the hydrogels.

Code	Polysaccharide type, %w	Water, % w	Medium type, %v	$CaCl_2$, mg/ml
dXG1-W	dXG, 1.0	99.00	\	\
dXG1-S	dXG, 1.0	49.00	SCM, 50	\
dXG1-C	dXG, 1.0	49.00	CDM, 50	\
dXG1-O	dXG, 1.0	49.00	ODM, 50	\
dXG2.5-W	dXG, 2.5	97.50	\	\
dXG2.5-S	dXG, 2.5	47.50	SCM, 50	\
dXG2.5-C	dXG, 2.5	47.50	CDM, 50	\
dXG2.5-O	dXG, 2.5	47.50	ODM, 50	\
kC1-W	kC, 1.0	99.00	\	\
kC1-S	kC, 1.0	49.00	SCM, 50	\
kC1-C	kC, 1.0	49.00	CDM, 50	\
kC1-O	kC, 1.0	49.00	ODM, 50	\
Alg1_2.5-W	Alg, 1.0	99.00	\	2.50
Alg1_2.5-S	Alg, 1.0	48.75	SCM, 50	2.50
Alg1_2.5-C	Alg, 1.0	48.75	CDM, 50	2.50
Alg1_2.5-O	Alg, 1.0	48.75	ODM, 50	2.50
Alg1_5-W	Alg, 1.0	99.00	\	5.00
Alg1_5-S	Alg, 1.0	48.50	SCM, 50	5.00
Alg1_5-C	Alg, 1.0	48.50	CDM, 50	5.00
Alg1_5-O	Alg, 1.0	48.50	ODM, 50	5.00
Alg2.5_5-W	Alg, 2.5	97.50	\	5.00
Alg2.5_5-S	Alg, 2.5	47.00	SCM, 50	5.00
Alg2.5_5-C	Alg, 2.5	47.00	CDM, 50	5.00
Alg2.5_5-O	Alg, 2.5	47.00	ODM, 50	5.00

Known volumes of the 2 %w and 5 %w dXG polymeric dispersions were gently mixed with the same volume, so in a 1:1 ratio, of water, or SCM, or CDMor with ODM to obtain the required final concentration of polymer of 1 % and 2.5 % and then incubated at 37 °C for 10 min before any further use. kC 2 %w were prepared by mixing the powder with water and stirring at 80 °C. Afterwards, it was mixed with the same volume, so in a 1:1 ratio, of water, or SCM, or CDM or with ODM at 50° to obtain the required final concentration of polymer of 1 % and brought to 37°.

Alg 2 %w and 5 %w solutions were prepared by mixing the powder with water and stirring at room temperature (25 °C). Afterwards, they were mixed with the same volume, so in a 1:1 ratio, of water, or SCM, or CDM or with ODM, all added with a solution of $CaCl_2$, to obtain the required final concentration of polymer of 1 % and 2.5 % and $CaCl_2$ of 2.5 mg/ml or 5 mg/ml .

Each individual system is named after as dXGx-z, kCx-z or Algx_y-z, where x indicates the final polymer concentration in weight percentage, y indicates the final $CaCl_2$ concentration in mg/ml and z is a letter referring to the mixing medium, in particular, W stands for water, S for SCM, O for ODM and C for CDM. Table 1 shows the composition of all investigated systems in terms of polymer concentration, volume percentage of the added medium, and $CaCl_2$ concentration.

The incubation times will be referred to as T0 for the systems that are analyzed soon after preparation, T7 and T21 stand for the system that are analyzed respectively after 7 and 21 days of incubation at 37 °C. The incubation conditions are the same described in Section 2.4.

2.4. Cells loading and incubation and viability analysis

SASCs cells were loaded on dXG systems loaded by mixing the 2 %w and 5 %w dXG polymeric dispersions with the same volume of SASC suspension in either SCM, CDM or ODM.

SASCs cells were loaded on kC systems by mixing, at 50 °C, 2 %w kC with the same volume of SASC suspension in SCM, CDM or ODM.

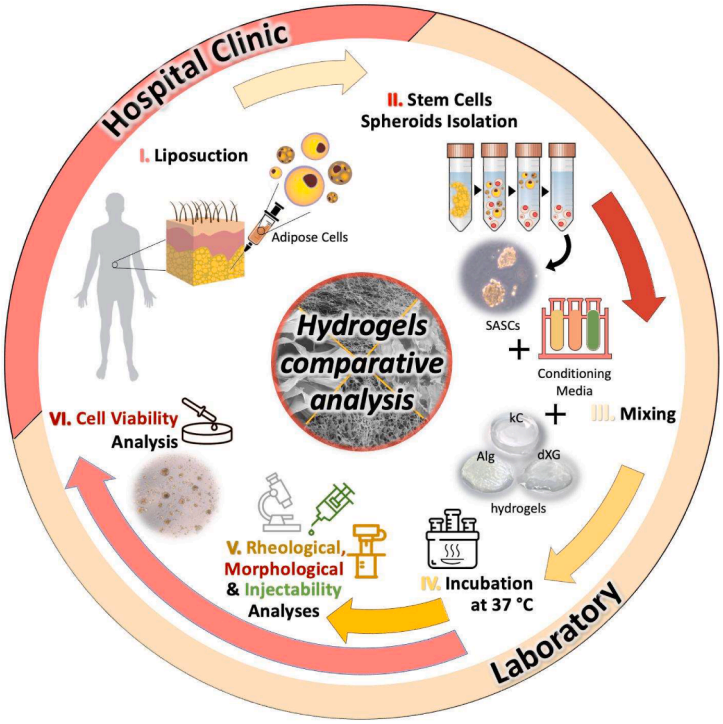

Fig. 1. Graphical representation of the experimental strategy. (I) Harvesting of adipose tissue by liposuction; (II) SASCs isolation and culturing in 3D conditions; (III) dXG, kC and Alg solutions mixing with either a stem cell medium (SCM), a chondro-inductive (CDM) or osteo-inductive medium (ODM), or with one of the media and SASCs; (IV) incubation of both SASC-free and SASC-laden hydrogels at 37 °C up to 21 days; (V) physicochemical, rheological, and morphological characterization of SASC-free systems; (VI) in-vitro evaluation of SASC-laden hydrogels.

SASCs cells were loaded on Alg systems by mixing 2 %w and 5 %w with the same volume of SASC suspension in SCM, CDM or ODM added with $CaCl_2$ to reach a $CaCl_2$ final concentration of 2.5 mg/ml or 5 mg/ml.

In all cases ca. 50000 cells/well were loaded (1:1 in a 1ml of final volume), in triplicate condition and maintained in CO_2 incubator at 37 °C for 7 days and 21 days. Cell proliferation was monitored under a light microscope (Leica DM IL LED Fluo) and quantified through MTS analysis (3- (4,5-dimethylthiazol-2-yl)-5-(3-carboxymethoxyphenyl)-2-(4-sulfophenyl)-2H-tetrazolium)(Promega). The absorbance at 490 nm was analysed at 7 days and 21 days of incubation (TECAN Spark 10 M).

Statistical significance was determined by one-way ANOVA text with Bonferroni post-test to compare all systems, calculated with GraphPrism5 software. P values less than 0.05 were considered significant as $P < 0.05$; $P < 0.01$; $P < 0.001$.

2.5. Swelling/erosion evaluations

For swelling tests, from the hydrogel produced with water, six small samples were obtained (ca. 0.5 ml). They were pre-weighed with a precision balance and immersed via glass cylinders with a porous bottom in 250 ml of PBS mixed with 0.02 % of NaN_3 at human body temperature (37 °C). Sample volume (V_{sample}) to media volume (V_{media}) ratio was $V_{sample}/V_{media}=0.002$.

Samples were taken out from the solutions at predetermined time intervals, carefully blotted and weighted. The solvent was not changed or reintegrated during the experiment. The Mass Change (%MC) was determined as:

$$MC = \frac{W_t - W_i}{W_i} \times 100$$

where W_t is the weight of the hydrogel at time t and W_i is the initial weight.

2.6. Small-angle oscillatory rheometry

The rheological analysis in small-oscillatory conditions was carried out using a stress-controlled Rheometer AR G2 (TA Instruments) with 20 mm diameter PIK anti-slippery plate and gap in the range 500-4000 μm. Strain sweep measurements were performed to explore the extension of the linear viscoelastic behavior strain range, at 1 Hz, and identify the optimum strain conditions for the subsequent frequency sweep tests. Frequency sweep measurements were also performed at constant strain in the range between 4×10^{-4} and 1×10^{-2}, depending on the system, and the frequency was swept between 0.1 Hz and 10 Hz. About 2 ml of each formulation were placed and the measurements started after 10 min of thermal and structural equilibration at the measurement temperature of 37.0±0.1 °C, controlled by a built-in Peltier system. Measurements were carried out in triplicate from independent preparations. The represented plots of *G'* and *G"* are the arithmetic average of the three curves.

2.7. Morphological analysis

Hydrogel microstructure was investigated using a Field Emission Scanning Electron Microscope (SEM) Phenom ProX desktop at an accelerating voltage of 10kV. The hydrogels were frozen in liquid nitrogen at -196 °C for 5 min, freeze-dried for 24 h, mounted on aluminum stubs and gold coated by JFC-1300 gold coater (JEOL) for 120 s at 30 mA before scanning.

2.8. Injectability

For injectability assessment of the Alg and dXG hydrogels formulated with SCM, force-displacement plots of formulations pre-loaded in syringes were carried out with an Instron Universal Uniaxial Testing Machine 3365 equipped with 1/1000 N load cell capacity, in compression mode, by applying a constant displacement rate (40 mm/min equivalent

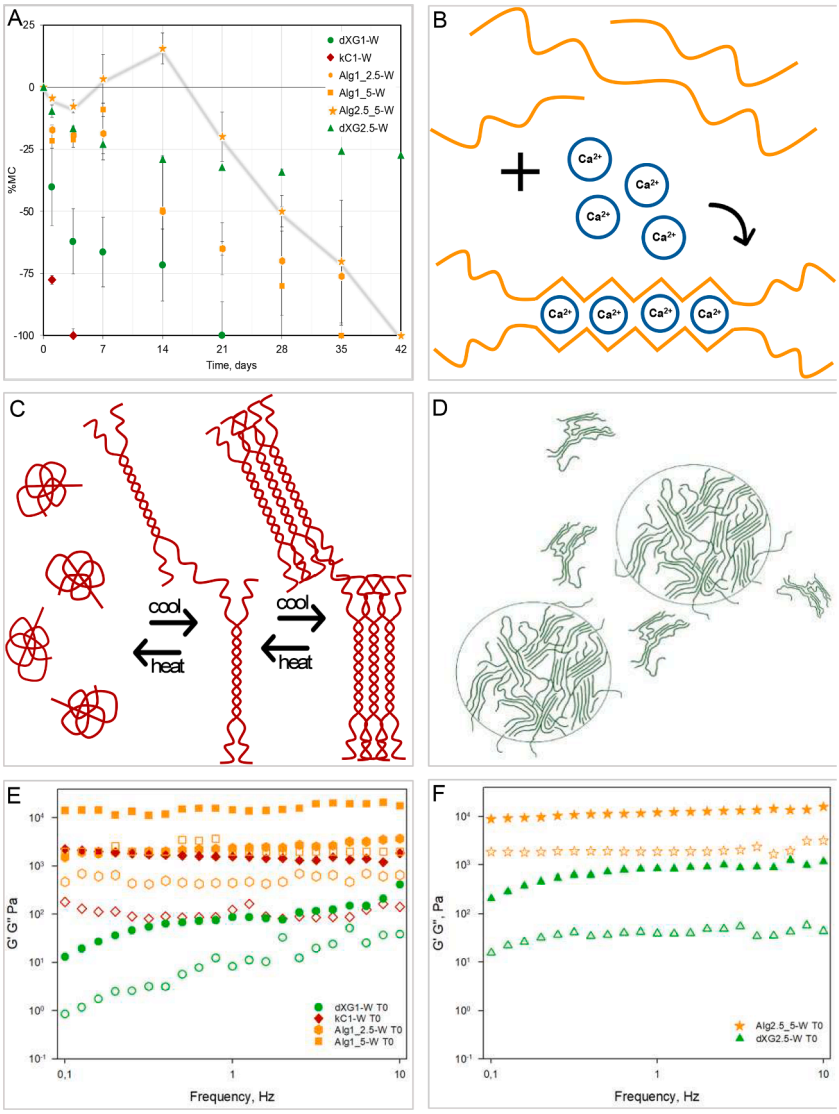

Fig. 2. A) Average mass change percentage (MC%) of Alg1_2.5-W, Alg1_5-W, dXG1-W, kC1-W, Alg2.5_5-W and dXG2.5-W hydrogels as a function of time; B) Alginate gelation mechanism as «eggbox»; C) Schematic illustration of the possible gelling mechanism of the carrageenan macro-molecules; D) The supramolecular organization of xyloglucan in water (Dispenza et al., 2020); Storage modulus, G' (full dot), and loss modulus, G'' (hollow dot) as function of frequency of E) T0 dXG1-W, Alg1_2.5-W, Alg1_5-W and kC1-W hydrogels as function of frequency; F) T0 Alg2.5_5-W and dXG2.5-W hydrogels at 37 °C.

to 5.30 mL/min) to the plunger of the syringe and measuring the resulting force (F) as function of the displacement, three times per system. The syringe was immobilized with a metal clamp. The injection was carried out with 2.5 ml polypropylene syringes equipped with a G23 needle. All experiments were performed after the systems were stored at 4 °C for 24 h and thermally equilibrated at room temperature (25 °C) for 1 h. The influence of the specific set up and the friction of the plunger was preliminarily evaluated by filling the syringe with water and extruding it in air. The plug force of the dispersions was measured by extrusion of the material in air or rabbit knee joint (KJ) or intra-muscle (IM). The results are expressed in terms of force, F, vs 1 – ε, that is the normalized travelled distance, where ε is representing the ratio (Td-D)/Td, where Td is the maximum distance the plunger can physically travel, and D is the distance travelled.

The following parameters were determined from the force-displacement plots: (i) the plunger-stopper break loose force (or "initial glide force"; PBF): the force required to initiate the movement of the plunger; (ii) the maximum force (F_{max}): the highest force measured before the plunger finishes its course at the front end of the syringe; (iii) the dynamic glide force (DGF): the force required to sustain the movement of the plunger to expel the content of the syringe. The experiments were performed in triplicate.

3. Results and discussion

The experimental strategy is graphically represented in Fig. 1. The three polysaccharides were individually dissolved in water at different concentrations and then mixed with water (W), a stem cell medium, a chondrogenic medium and osteoblastic differentiation medium at 50 % v.

When SASCs were embedded, they were dispersed in each of the three solutions that were added to the aqueous polymer dispersion.

Both SASC-free and SASC-laden hydrogels were incubated at 37 °C for up to 21 days. SASC-free systems were characterized for their mechanical properties by small amplitude oscillatory rheological measurements soon after being formulated (T0), after 7 days (T7), and 21 days (T21) of incubation and for their morphology by Scanning Electron Microscopy at T0 and T21. The swelling and erosion behavior of the systems was investigated by measuring weight changes upon immersion in a large volume of isotonic phosphate buffer at 37 °C to test the

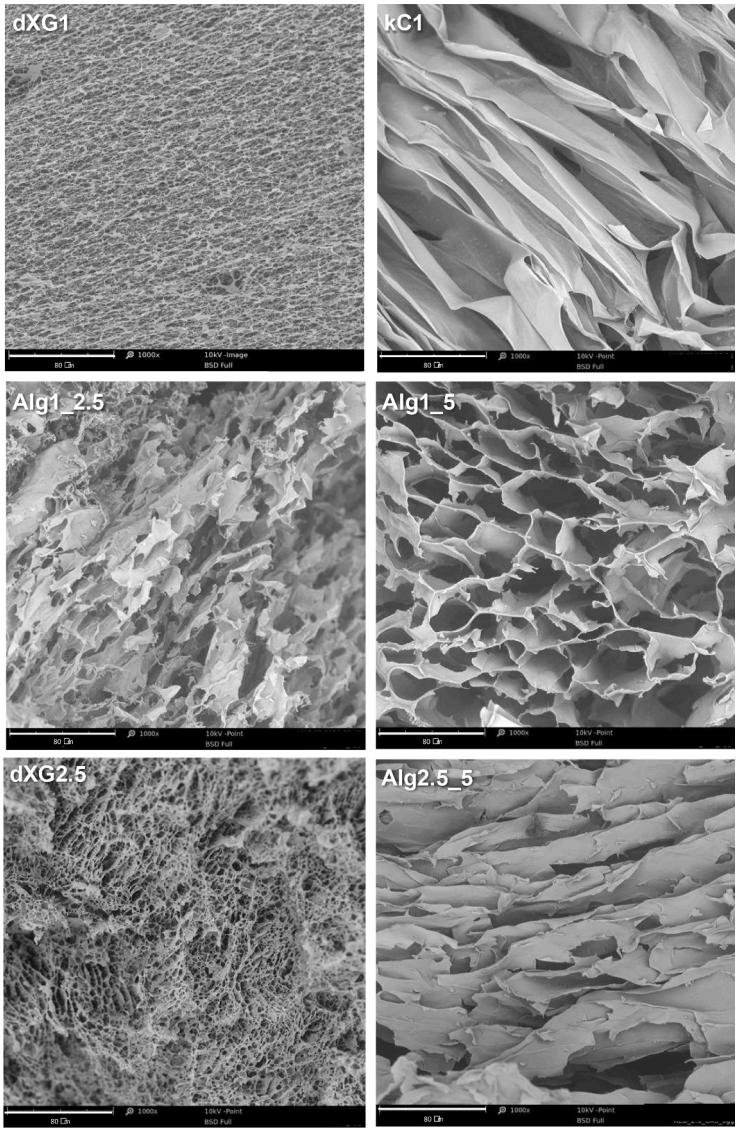

Fig. 3. SEM micrographs (cross-sections) of dXG1, kC1, dXG2.5, Alg1_2.5, Alg1_5 and Alg2.5_5 hydrogels conditioned with water at T0 (scale bar 80 μm). Magnification 1000X.

network strength. All SASC-laden hydrogels were evaluated for cell viability at T0, T7 and T21. Finally, the injectability of selected formulations was also evaluated by force-displacement measurements to assess the translation potential of these systems.

3.1. Preliminary screening of hydrogels using water as solvent and swelling medium

Based on the results of previous studies dXG gels were produced by mixing 2 % and 5 % aqueous dispersions of dXG with 50 %v water (Muscolino et al. 2021).

When using alginate, a preliminary screening was performed to identify the Ca^{2+} concentration that can induce gelation of Alg when the final polymer concentration is 1 %w or 2.5 %w, as for dXG. The range of Ca^{2+} concentration explored was from 1.25 mg/ml to 5 mg/ml. Photographs of the alginate gels after preparation, and after 1 and 6 weeks of storage at room temperature (25 °C) are shown in **Figure S2** of Supporting material. Homogenous wall-to-wall gels were obtained with both 2.5 mg/ml and 5 mg/ml $CaCl_2$ when Alg concentration was 1 %w, and with 5 mg/ml when Alg concentration was 2.5 %w. Decreasing Alg concentration below 1 %w did not result in macroscopic gelation, while increasing it above 2.5 %w resulted in systems that formed gels too quickly and left no time for mixing with the cells. From these preliminary results, three systems were selected to be then formulated with the instructive media: 1 % Alg with 2.5 mg/ml and 5 mg/ml $CaCl_2$ and 2.5 % Alg with 2.5 mg/ml $CaCl_2$.

For kC, the polymer concentration also controls the sol-gel transition temperature; willing this temperature to be lower than 50 °C, the final kC concentration could not be higher than 1 %w. Concentrations lower than 1 %w did not yield wall-to-wall gels.

To understand the nature and strength of the networks that the five formulations can form, without the perturbation of the various solutes present in the "instructive" media, the swelling/erosion and rheological frequency curves, as well as the morphology of the systems formulated with water alone, were compared. The hydrolytic stability of the hydrogels was evaluated by immersing cylindrical samples of each system in isotonic phosphate buffer at pH 7.4 and 37 °C. In Fig. 2A the average mass change as function of the immersion time is reported. dXG1-W loses weight until complete dissolution in nearly three weeks. dXG2.5-W slowly erodes during the first three weeks until it reaches a plateau. kC1-W completely dissolves in a few days. Alg1_2.5-W gradually dissolves until it reaches complete dissolution after about 40 days,

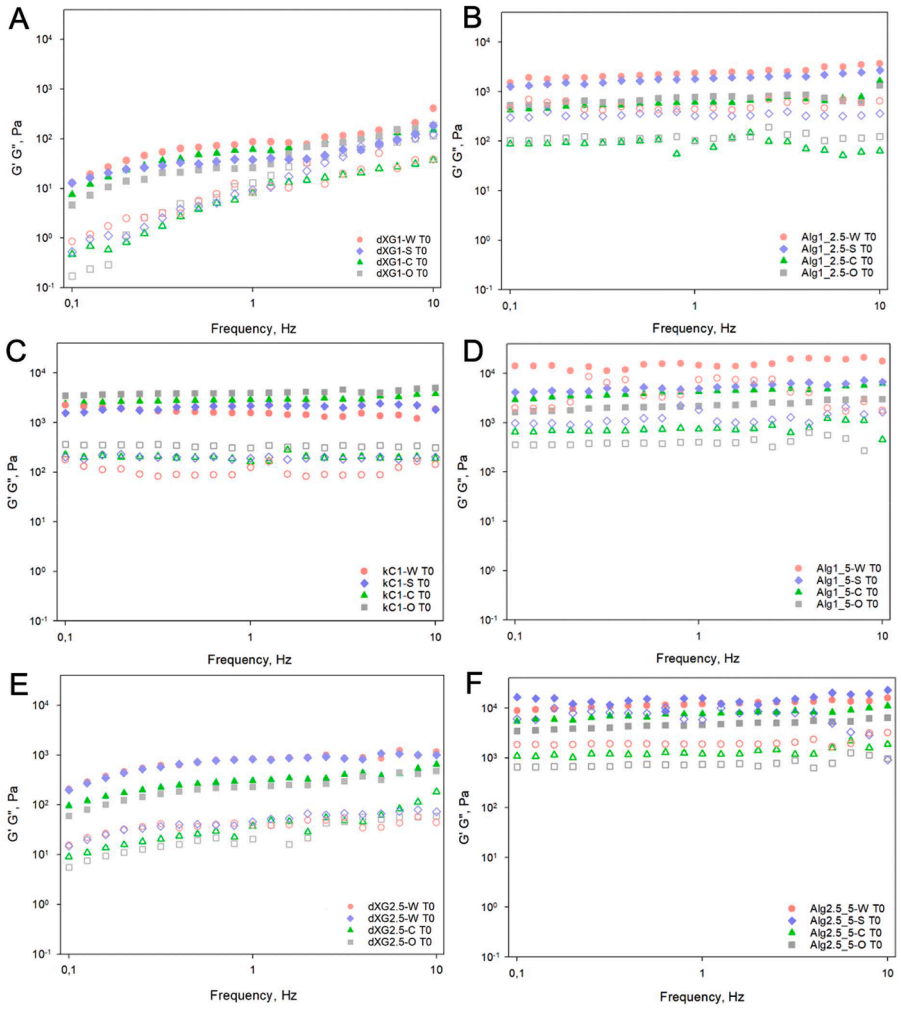

Fig. 4. Storage modulus, G' (full dot), and loss modulus, G" (hollow dot), of dXG1 (A), Alg1_2.5 (B), kC1 (C), Alg1_5 (D), dXG2.5 (E) and Alg2.5_5 (F) hydrogels conditioned with water, SCM, CDM, and ODM at T0.

while Alg1_5-W and Alg2.5_5-W first lose weight, then swell and finally dissolve after about 30 days.

The different behavior of the hydrogels produced with different biopolymers can be explained considering their different gelation mechanism and the nature of the crosslinking points that are represented in Fig. 2B-D, while the chemical structure of all three polysaccharide is presented in **Figure S3** of Supporting material. Both Alg and kC hydrogels crosslink through ion-mediated chain association. Specifically, in Ca-alginate systems, gelation begins with ion exchange between Na^+ and Ca^{2+} that leads to the formation of chelating boxes (the widely reported egg-box structure) that glue two consecutive G units of two alginate chains through a coordinated Ca^{2+} cation (Fig. 2B). Subsequently, dimer association occurs through water-mediated hydrogen bonding and disordered ionic interaction. Gelling can proceed through further intra-cluster associations at the expense of side packing (Rinaudo, 1993). When immersed in a large excess of salt solution, an exchange of ions from Ca^{2+} to Na^+ occurs, recreating conditions for solvation of the polymer chain. This may cause initial weight gain due to water absorption until polymer erosion prevails, compromising the integrity of the network. For kC, cations of specific size and charge, such as K^+, are required to perfectly screen the fixed negative charges in the polymer, filling the gaps of double and triple helices (Fig. 2C). When the gels form in the absence of these ions, as in our case, charge screening is only due ionic impurities present in the system. For this reason, the network is not very resistant to erosion (J. Liu et al., 2015; Mangione et al., 2003). Unlike the other two polymers, dXG is a nonionic polymer; the cross-linking points consist of condensed domains of chains organized in ribbons (Fig. 2D) (Dispenza et al., 2020). The driving force behind self-assembly is the hydrophobic interaction; segments stripped from side branches (that is why the polymer is partially degalactosylated) associate and establish multiple hydrogen bonds (Dispenza et al., 2020). When most of the chains have segments involved in at least one condensed domain, as in the case of dXG2.5, the network survives erosion and the initial mass reduction is due to elution of the fraction of free or only weakly bound chains.

The mechanical spectra of the various systems are shown in Fig. 2E and F. The four systems with 1 %w polymer concentration show G' and G" curves that span over three orders of magnitude. Alginate, that among the three polymers has the lowest molecular weight, when formulated with 5 mg/ml $CaCl_2$ presents the highest values of elastic modulus, that is also frequency-independent and almost one order of magnitude higher than the corresponding values of loss modulus. From its viscoelastic response, it can be described as a strong gel. Reducing salt concentration reduces the strength of the alginate gel as it reduces the cross-linking density. Alg1_2.5-W has one order of magnitude lower elastic modulus, that is comparable to that of kC1-W, although the latter has much lower G" values, reflecting a more brittle behavior. dXG has the lowest G' and G" curves, with a significant frequency-dependence. dXG gelation leads to the formation of relatively heterogeneous networks, in terms of mesh size and crosslinking density. This explains the wide range of relaxation times and the frequency-dependence of G' and G" curves. Increasing the polymer concentration causes a modest

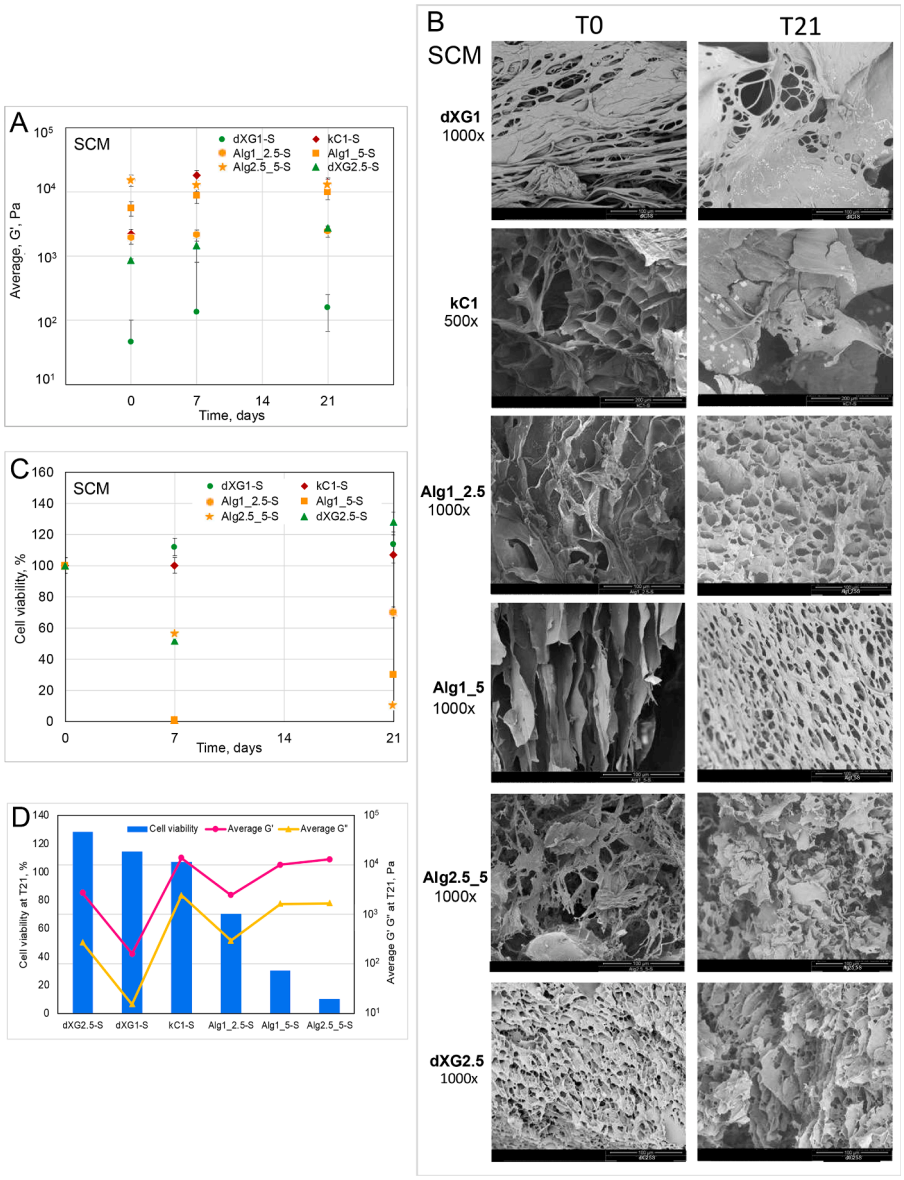

Fig. 5. A) Average G′, of hydrogels conditioned with SCM at T0, T7 and T21; B) SEM micrographs (cross-sections) of hydrogels conditioned with SCM at T0 and T21; Magnification 1000X for all except for kC 500X. C) cell viability of SASCs in hydrogels as a function of time at T7 and T21 in SCM of *in vitro* culture; D) Average G′ and G", of hydrogels conditioned with SCM at T21 and cell viability of SASCs in hydrogels as a function of time at T21 of *in vitro* culture. All systems (except dXG1-S vs kC1-S that were not significant) were significant as $P < 0.001$ and dXG2.5-S vs dXG1-S as $P < 0.01$.

increase of G' and G" curves of dXG2.5-W, that become less frequency sensitive, indicative of a more uniform network. The increase of polymer concentration with the same Ca^{2+} concentration, when we compare Alg2.5_5-W to Alg1_5-W, does not significantly modify storage and loss moduli. This means that the crosslinking density of the network is not appreciably affected by the increase of polymer concentration probably because the Ca^{2+} concentration has not been increased proportionally.

Fig. 3 displays the cross-sectional morphologies of all systems. dXG1-W shows a uniform 3D network of small, interconnected pores (~ 5 μm), that seems formed by very thin shreds of torn and stretched membranes. Alg1_2.5-W also shows a porous microstructure, with irregularly sized pores and thicker walls. In some regions, shredded membranes are also evident. In contrast, Alg1_5-W shows a much more regular and porous architecture, with average pore size of 40 μm. kC1-W shows a completely different microstructure, consisting of stacked lamellae, fused in places, which is in good agreement with the suggested low crosslinking density. This morphology is quite like that of Alg2.5_5-W. dXG2.5-W is also characterized by a morphology like that of dXG1-W, only with thicker polymer walls. Again, the difference in the morphology is more obvious between dXG and the other two polymers, reflecting different network structures and gelation mechanisms.

3.2. *Influence of instructive media composition on hydrogel mechanical properties*

The influence of the instructive media composition on the initial network organization was investigated. Fig. 4 shows the rheological behavior in small amplitude oscillation conditions of all systems at T0. The curves relative to water are also reported, for comparison. For all systems, *G'* curve is higher than *G"*, indicating that in none of the cases gelation is prevented.

For dXG1 systems (Fig. 4A) both *G'* and *G"* plots are frequency dependent. Systems mixed with media have lower moduli than those mixed with water. This suggests that the solutes in the media behave as chaotropes, destabilizing hydrophobic aggregates.

The instructive media, particularly ODM and CDM, affect also Alg1-

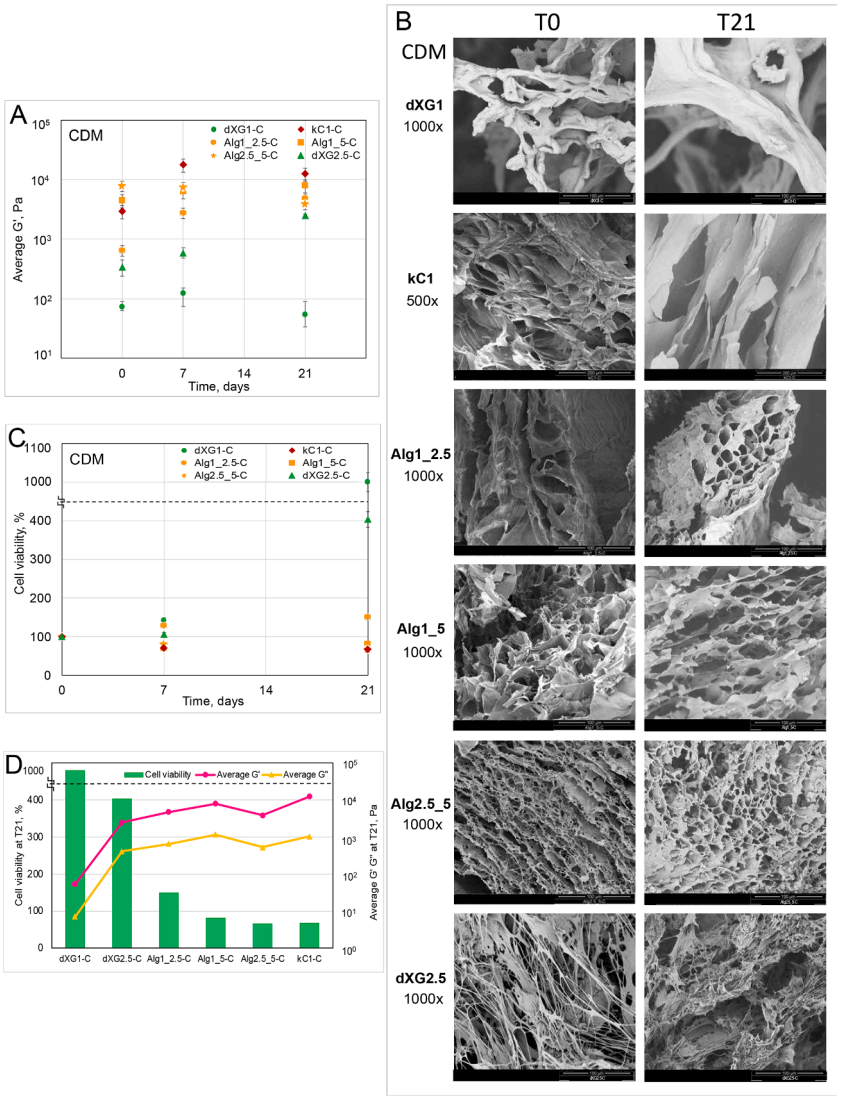

Fig. 6. A) Average G′, of hydrogels conditioned with CDM at T0, T7 and T21; B) SEM micrographs (cross-sections) of hydrogels conditioned with CDM at T0 and T21. Magnification 1000X for all except for kC 500X.; C) cell viability of SASCs in hydrogels as a function of time at T7 and T21 in CDM of *in vitro* culture; D) Average G′ and G", of hydrogels conditioned with CDM at T21 and cell viability of SASCs in hydrogels as a function of time at T21 of *in vitro* culture. All systems (except Alg2.5_5-C vs kC1-C that were not significant) were significant as $P < 0.001$ and Alg2.5_5-C vs Alg1_5-C/ Alg1_5-C vs kC1-C as $P < 0.05$.

based systems (Fig. 4B and D). The most obvious case is that of Alg1_5 (Fig. 4D), which sees reductions in storage modulus of up to an order of magnitude. For kC systems, the opposite effect is observed, as the system formulated with water has the lowest moduli. ODM and CDM have a slight strengthening effect, while the effect of SCM is almost negligible. Less pronounced effects are shown by the two hydrogels with the highest polymer concentration, dXG2.5 (Fig. 4E) and Alg2.5_5 (Fig. 4F), as expected.

3.3. SASCs-laden hydrogels formulated to preserve cell stemness

To understand how the mechanical and morphological properties of the hydrogels formulated with SCM, a medium developed to preserve stem cell conditions (Di Stefano et al., 2016), influence cell survival, viability data were collected over a three-week period on SASCs-laden hydrogels and were supported by rheological and SEM analyses carried out on cell-free hydrogels incubated for the same time under the same conditions. Fig. 5A and Fig. 5C show the average storage modulus in the 0.5 Hz–5 Hz interval and the cell viability results for all systems at T0, T7 and T21, respectively. Fig. 5B shows the cross-sectional morphologies at T0 and T21. The full mechanical spectra (G' and G" curves as function of frequency) at T0, T7 and T21 are reported in the supporting materials, **Figure S4-S10**.

Both dXG systems start with the lowest G' modules, which increase with time, such that dXG2.5-S and Alg1_2.5-S have comparable G' values at T21. The increase of G' (and G") values with time for dXG2.5 can be explained with a slow network reorganization, after the initial rapid gelation. Indeed, for dXG2.5-S, the G' and G" curves become nearly independent of frequency, sign of the formation of a stronger gel with a more uniform network structure (Figure S8). For kC1-S both storage and loss modulus plots increase after 7-day incubation and remain more or less invariant after two further weeks of incubation. This could be due to the involvement of K^+ cations from medium and consequent expulsion of syneresis water during the first 7 days, after that the system reaches a pseudo-equilibrium. The alginate substrates exhibit intermediate moduli that do not significantly vary over time. Comparison of the morphologies at T0 and T21 provides insights to interpret the differences observed in the mechanical spectra (Fig. 5B). An overall examination of the morphologies at T0 reveals that the dXG and kC systems are the most affected, while the Alg systems are much less so. On the other hand, the latter systems were the only ones to which a crosslinking agent ($CaCl_2$) was specially added, so they are the least

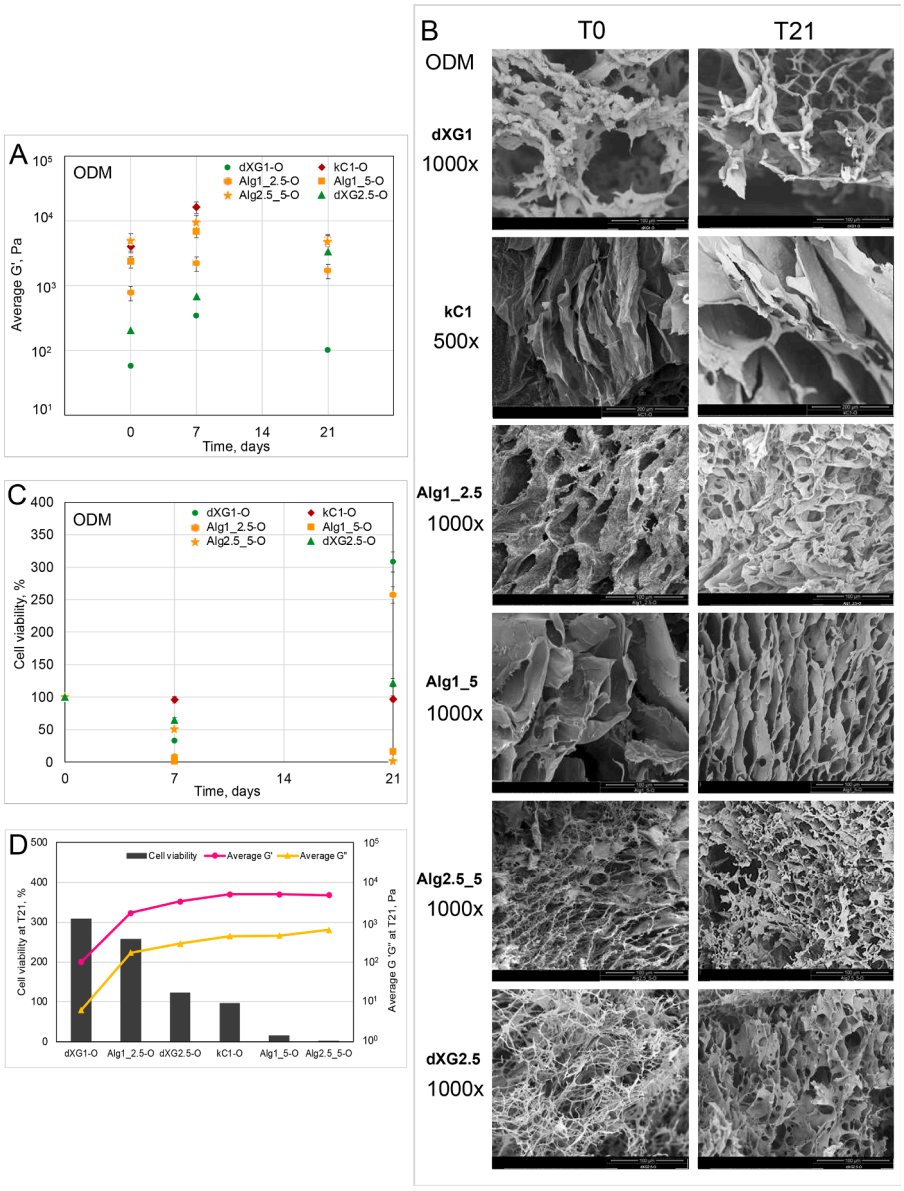

Fig. 7. A) Average G′, of hydrogels conditioned with ODM at T0, T7 and T21; B) SEM micrographs (cross-sections) of hydrogels conditioned with ODM at T0 and T21; Magnification 1000X for all except for kC 500X. C) cell viability of SASCs in hydrogels as a function of time at T7 and T21 in ODM of *in vitro* culture; D) Average G′ and G", of hydrogels conditioned with ODM at T21 and cell viability of SASCs in hydrogels as a function of time at T21 of *in vitro* culture. All systems were significant as $P < 0.001$ and Alg2.5_5-O vs Alg1_5-O as $P < 0.05$.

sensitive to changes in medium composition. The dXG1-S system has an architecture formed by thicker beads and interconnected open pores at T0, which develops even larger cavities and large membrane surfaces at T21. The structure partially collapses with lyophilization. kC1-S T0 shows an irregular honeycomb-type porous structure, different from the layered lamellae of the kC1-W T0. At T21 the morphology has evolved towards the formation of membranes that collapse and break upon freeze drying. Interestingly, all alginate systems show morphologies at T21 that more closely resemble those of the system with water at T0, as if with time the initial interference of other solutes in the instructive medium had been compensated for and the calcium ions had time to migrate and form a more organized structure. This could explain the less frequency-dependent behavior of the mechanical spectra and the small variations in the value of the moduli.

A quantitative analysis of cell viability was performed by MTS analysis (Fig. 5C). The results in stemness conditions at 7 days shows decreased viability of the cells for four systems; all the alginate formulations and dXG2.5. Cell viability is not varied kC1-S and slight proliferation is seen for dXG1. This behavior could be attributed to perturbations of the spheroids caused by free calcium cations in the alginate formulations and, more generally, to too rapid gelation that does not promote uniform distribution of the spheroids within the hydrogels and their nesting in the hydrogel. Interestingly, in most of the cases, the cells that remained viable proliferated from T7 to T21. This behaviour was unexpected considering that SASCs in SCM medium are in a quiescent state of the cell cycle. The system that stimulated most the proliferation was dXG2.5. A T21, this last hydrogel was the one that reached the highest values of cell viability.

When comparing the G' and G" values to the cell viability data at T21 (Fig. 5D) we do not see a strong correlation. This suggests that other features of the niche, and most probably the chemical structure of the polymers, play a more important role than just the viscoelasticity of the network. Indeed, the dXG systems appear to be the best not only to preserve stem cell viability but also to support their expansion.

3.4. SASCs-laden hydrogels formulated to stimulate chondrogenic differentiation

The same analyses described above were performed for the systems prepared with CDM, a medium that stimulates chondrogenic differentiation. The results from the rheological analysis (Fig. 6A and **Figure S4-S10** of supporting information) show that also in this case the dXG hydrogels are the ones that present the lowest moduli. For dXG1-C, G' and G" increased at T7 but at T21 both decreased, probably due to phase segregation phenomena. In contrast, dXG2.5-C shows a gradual increase in modules from T0 to T21 and its final values are similar to the ones of dXG2.5-S at T21. kC1-C starts with lower moduli but reaches the highest values after 7 days, as in the case for SCM. The alginate hydrogels have average moduli intermediate among those of the other systems, increasing only with calcium concentration and over time with the exception of the system with the highest polymer concentration, that ends up having the lowest moduli among the three.

The morphology evolution of the systems is shown in Fig. 6B. dXG1-C shows big pores and thick walls that increase in size and thickness over time; that could explain the decrease in moduli in the mechanical spectra. kC1-C T21 shows layered lamellae. The more packed architecture than in dXG1-C explains the higher moduli. Alg1_2.5-C T21 shows a very similar morphology to Alg1_2.5-C T0 with small pores, thicker and more structured lamellae. This could account for the less frequency-dependent behavior of the mechanical spectra and the increase in moduli. Alg2.5_5-C T0 shows a porous structure that evolves to bigger pores at T21, possible indication of an erosion of the material that explains the deterioration of mechanical properties with time. dXG2.5-C T0 morphology shows fusion of ribbons and fibrils and evolves towards membrane with pores and thicker walls, also in good agreement with the mechanical spectra.

Cell viability data are shown in Fig. 6C. Differently from SCM, in CDM we do not witness to significant mortality at T7. On the contrary there is a slight increase of viability for dXG1 and Alg1_2.5, no change for dXG2.5 and a slight decrease to 70 % for Alg1_5-C and Alg2.5_5-C. At T21, cells continue to proliferate in dXG hydrogels with an overall ~ 10-fold increase in viability for dXG1-C and ~4-fold for dXG2.5-C. The other systems show the same values at T21. Even with CDM, the dXG hydrogels outperform the others.

In this case though, when comparing the average G' and G" with the cell viability (Fig. 6D) a good correlation is shown, with proliferation being higher the lower are the G' and G". Several groups report that when MSCs are seeded on the surface of the hydrogels, they show lineage specification depending on the substrate mechanics (Burdick & Vunjak-Novakovic, 2009; J. F. Liu et al., 2011). Here, in the presence of differentiation inducing soluble factors, the lower G' and G" appear to offer optimal conditions to preserve the cell viability and stimulate proliferation.

3.5. SASCs-laden hydrogels formulated to stimulate osteoblastic differentiation

The results obtained with ODM, the medium that stimulates osteogenic differentiation, are shown in Fig. 7 and Figure S4-S10 of the supporting information.

Fig. 7A shows the average G' as a function of time for all systems. With the noticeable exception of dXG2.5, all systems see an initial increase of G' at T7 and a decrease at T21 to come back to values that are not so different from the initial values at T0. The morphology evolution of the systems is showed in Fig. 7B. Differently from the formulations with SCM or CDM, and in good agreement with the viscoelastic properties, also the evolution of the morphology is small. Only the dXG2.5-O initially shows a very delicate and intricate filament structure that develops at T21 into a more robust structure with bigger pores and thicker walls. The MTS analysis (Fig. 7C) at T7 showed a decrease in cell viability in all hydrogels with the exception of kC1-O. dXG1-O and Alg 1_5-O that reached a residual viability of 70 % and 10 % recovered to a final overall ~3-fold increase and 2.5-fold increase at T21, respectively. Also dXG2.5 showed proliferation from T7 to T21 but less pronounced. In kC1-O cell viability was unvaried during the whole period of observation.

Table 2
PBF, F_{max} and DGF_{av} values for dXG1-S, Alg1_2.5-S, and dXG2.5-S.

Systems	PBF [N]	F_{max} [N]	DGF_{av} [N]
dXG1-S 23G	3.3	8.34	5.2
dXG1-S 23G KJ	10	11	9.4
dXG1-S 23G IM	7.4	22.8	17.7
Alg1_2.5-S 23G	6	17.6	7.7
Alg1_2.5-S 23G KJ	5.2	5.7	4.3
Alg1_2.5-S 23G IM	7	15.8	10.7
dXG2.5-S 23G	17	20.5	15.7
dXG2.5-S 23G KJ	15	21.5	17.1
dXG2.5-S 23G IM	12	16	15.2

When comparing average G' and G" values with cell viability values at T21 (Fig. 7D), we observe a good correlation; systems that have the lower G' and G" moduli also in this case are those that lead to the highest viability values at T21. In this case, one of the alginate systems, Alg1_2.5 outperform dXG2.5. Among all the systems, this is the one with the lowest content of Ca^{2+} ions. We can argue that the presence of free Ca^{2+} during the ion exchange with Na^{+} of alginate can contribute providing suitable conditions for osteoblast proliferation. The work of S. Maerno et al. has shown that 2–4mM Ca^{2+} is suitable for proliferation and survival of osteoblasts. Slightly higher concentrations (6–8 mM) favor osteoblast differentiation and matrix mineralization. Even higher concentrations (>10mM) are cytotoxic (Maeno et al., 2005).

The fact that softer hydrogels, despite being based on xyloglucan or alginate, support SASCs viability and proliferation when incubated with an osteogenic differentiative medium is not at all unexpected. Although many studies report that osteogenic differentiation is enhanced on a stiffer substrate (Shih et al., 2011; Witkowska-Zimny et al., 2013), Žigon-Branc et al. (Žigon-Branc et al., 2019) report that softer hydrogels, made of methacrylamide-modified gelatin (G' ~0.5 kPa), better support both chondrogenic and osteogenic differentiation of stem cell spheroids (hASC/hTERT). This could be due to a more favorable environment for 3D encapsulation, that ensures adequate spheroid spacing.

3.6. Injectability of Hydrogels

The ease of injection (injectability) of the different hydrogels, which have already been evaluated for their ability to preserve stem cell viability and promote differentiation and proliferation, was tested, with the prospect of their use for the repair of chondroarticular defects. Injectability can be influenced by the geometry of the needle, i.e., its inner diameter, length, shape of the opening, and syringe material of the syringe. Common needle configurations for articular injection of viscous formulations are 21 G and 23 G (Stephens et al., 2008). he tests were conducted using SCM as the mixing medium, considering that once the stem cells were injected, the cells themselves would be able to pick up stimuli from the environment to differentiate into the necessary lineage for the damaged tissue. Injections were performed with a 23 G needle, and force-displacement graphs were recorded during extrusion into air, injection into the rabbit knee joint (KJ) and injection inside the muscle (IM).

Injectability parameters, like plunger-stopper break loose force (PBF), maximum force (F_{max}), and dynamic glide force (DGF_{av}), were analyzed and presented in Table 2. Force-displacement plots, obtained applying a constant displacement rate to the plunger of the syringe and measuring the resulting force as function of the displacement, are provided in Fig. 8. The formulations tested were those that gave the best results in terms of stem cell viability and proliferation both in chondrogenic and osteogenic media; namely, dXG1, dXG2.5 and Alg1_2.5

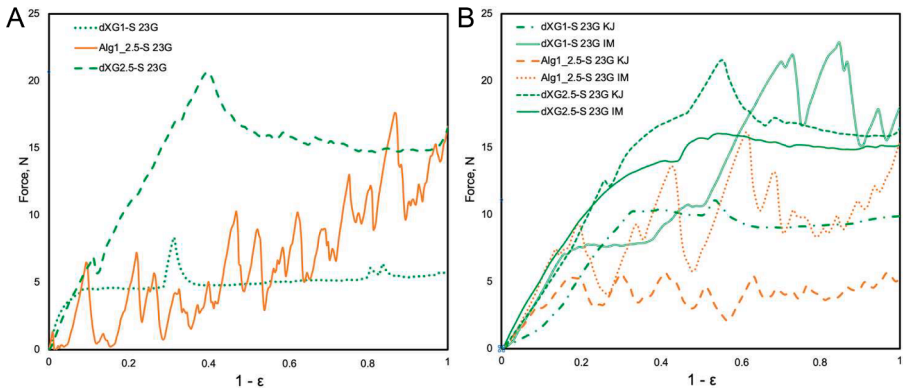

Fig. 8. Force required to expel the fluid (N) as a function of the normalized travelled distance, at the crosshead speed of 40 mm/s, in air of dXG1-S, Alg1_2.5-S and dXG2.5-S dXG1-S, Alg1_2.5-S and dXG2.5-S (A) and rabbit knee joint (KJ) and intra-muscle (IM) of dXG1-S, Alg1_2.5-S and dXG2.5-S hydrogels (B).

(Fig. 8A). With 23 G needle, dXG1-S was extruded in air with a relatively constant, low ejection force. Alg1_2.5-S initially ejected syneresis water, then the material was extruded with progressively greater force. The extruded material was inhomogeneous, as also revealed by the force vs normalized travelled distance plot. The dXG2.5-S 23G initially required a steadily increasing force to reach the maximum, then progressed with a constant force.

Injections into rabbit knee joint and intra-muscle mimic different tissue resistances. dXG1-S KJ showed higher resistance than in air, Alg1_2.5-S KJ exhibited lower resistance, dXG2.5-S KJ demonstrated comparable resistance (Fig. 8B). It can be highlighted that all systems require a force to be injected that is well below the medical operator average maximum force, estimated equal to 79.8 N (Vo et al., 2016), but also below the most conservative maximum acceptable injection force for non-medical operators of 40 N (Watt et al., 2019).

4. Conclusions

Hydrogels based on dXG had shown very promising properties for their ability to preserve the stemness of human adipose stem cell spheroids and support their differentiation into chondrocytes or osteoblasts. We wondered whether hydrogels stiffer than those of dXG could provide additional biomechanical cues that could promote cell attachment and proliferation. kC and Alg form hydrogels at concentrations similar to those of dXG, but through different mechanisms, so that they have higher stiffness than dXG. In general, the dXG substrates had lower G' and G" moduli than the Alg- and kC-based hydrogels. Another notable similarity was the ability of kC1 and both dXG systems to remodel themselves upon dynamic and reversible bond breaking/reforming. The Alg hydrogels were, in general, less affected by the composition of the incubation media and time, because they were formulated with an ionic crosslinker. The most interesting features of the SASCs-loaded hydrogels observed were the ability of kC1 to ensure 100 % viability of SASCs in SCM and of dXG1 to support their slight expansion. The dXG2.5-S system, which caused an initial decrease in viability, probably due to the poor ability of dXG jammed at 2.5 %w to ensure even distribution and optimal nesting of SASCs prior to gelation, on the longer time scale was able to support significant expansion of stem cells. Alginate-based substrates did not promote cell viability when incubated with SCM. This may be due to their rapid gelation and reduced remodeling capacity or the presence of free Ca^{2+}. Under chondrogenic and osteogenic differentiation conditions, a good correlation was found between cell viability and scaffold modules; the lower the G' and G", the higher the cell viability. The results confirmed the better performance of dXG1. It was also interesting to observe that under chondrogenic differentiation conditions SASCs never experienced complete mortality. One possible explanation could lie in the increased commitment of SASCs to the chondrogenic lineage. This hypothesis requires further investigation to be supported. In summary, the gelation mechanism and the ability of the network to nest spheroids and remodel over time, rather than the stiffness of the hydrogel, seem to be the most important feature of these artificial niches.

CRediT authorship contribution statement

Emanuela Muscolino: Writing – original draft, Visualization, Methodology, Investigation, Conceptualization. **Anna Barbara Di Stefano:** Writing – original draft, Visualization, Methodology, Investigation, Funding acquisition, Conceptualization. **Francesca Toia:** Writing – review & editing, Supervision, Resources. **Daniela Giacomazza:** Writing – review & editing, Supervision, Funding acquisition. **Francesco Moschella:** Writing – review & editing, Supervision. **Adriana Cordova:** Writing – review & editing, Supervision, Resources, Funding acquisition. **Clelia Dispenza:** Writing – review & editing, Validation, Supervision, Funding acquisition, Conceptualization.

Declaration of competing interest

The authors declare that they have no known competing financial interests or personal relationships that could have appeared to influence the work reported in this paper.

Data availability

Data will be made available on request.

Perspectives

Inductive media will be optimized to replace commercial media and be suitable for *in vivo* use. The ease of injection of dXG formulations is an important property to validate dXG-based hydrogel vectors for stem cell therapy of osteochondral defects and a variety of tissue engineering applications. Future research should focus on enhancing the biomechanical properties of these hydrogels to better mimic natural ECM, potentially by incorporating dynamic and responsive elements that further support cell proliferation and differentiation. Additionally, exploring the effects of varying Ca^{2+} concentrations and other biochemical cues could lead to more tailored and effective treatments for specific tissue engineering applications. Finally, from these results, generally dXG remains the best substrate for cell viability and differentiation. Other hydrogels, like the Alginate-based, can be optimised for specific biomedical applications.

Funding sources

Clelia Dispenza, Anna Barbara Di Stefano and Adriana Cordova were funded by the "Sicilian MicronanoTech Research And Innovation Center" - SAMOTHRACE – (B73C22000810001 - ECS_00000022) Spoke 3, and Emanuela Muscolino has received funding from the European Union - NextGenerationEU through the Italian Ministry of University and Research under PNRR - M4C2-I1.3 Project PE_00000019 "HEAL ITALIA" CUP B73C22001250006. The views and opinions expressed are those of the authors only and do not necessarily reflect those of the European Union or the European Commission. Neither the European Union nor the European Commission can be held responsible for them.

Acknowledgments

Authors wish to thank ATeN Center of University of Palermo,"Preparazione e Analisi dei Biomateriali" laboratory, for technical support.

Supplementary materials

Supplementary material associated with this article can be found, in the online version, at doi:10.1016/j.carpta.2024.100566.

References

Adebowale, K., Gong, Z., Hou, J. C., Wisdom, K. M., Garbett, D., Lee, H., Nam, S., Meyer, T., Odde, D. J., Shenoy, V. B., & Chaudhuri, O. (2021). Enhanced substrate stress relaxation promotes filopodia-mediated cell migration. *Nature Materials, 20*(9), 1290–1299. https://doi.org/10.1038/s41563-021-00981-w

Aguado, B. A., Mulyasasmita, W., Su, J., Lampe, K. J., & Heilshorn, S. C. (2012). Improving viability of stem cells during syringe needle flow through the design of hydrogel cell carriers. *Tissue Engineering Part A, 18*(7–8), 806–815. https://doi.org/10.1089/ten.tea.2011.0391

Bahram, M., Mohseni, N., & Moghtader, M. (2016). An introduction to hydrogels and some recent applications. In S. B. Majee (Ed.), *Emerging Concepts in Analysis and Applications of Hydrogels*. InTech. https://doi.org/10.5772/64301.

Brun-Graeppi, A. K. A. S., Richard, C., Bessodes, M., Scherman, D., Narita, T., Ducouret, G., & Merten, O.-W. (2010). Study on the sol–gel transition of xyloglucan hydrogels. *Carbohydrate Polymers, 80*(2), 555–562. https://doi.org/10.1016/j.carbpol.2009.12.026

Burdick, J. A., & Vunjak-Novakovic, G. (2009). Engineered microenvironments for controlled stem cell differentiation. *Tissue Engineering Part A, 15*(2), 205–219. https://doi.org/10.1089/ten.tea.2008.0131

Chen, D., Guo, P., Chen, S., Cao, Y., Ji, W., Lei, X., Liu, L., Zhao, P., Wang, R., Qi, C., Liu, Y., & He, H. (2012). Properties of xyloglucan hydrogel as the biomedical sustained-release carriers. *Journal of Materials Science: Materials in Medicine, 23*(4), 955–962. https://doi.org/10.1007/s10856-012-4564-z

Chen, S.-C., Wu, Y.-C., Mi, F.-L., Lin, Y.-H., Yu, L.-C., & Sung, H.-W. (2004). A novel pH-sensitive hydrogel composed of N,O-carboxymethyl chitosan and alginate cross-linked by genipin for protein drug delivery. *Journal of Controlled Release, 96*(2), 285–300. https://doi.org/10.1016/j.jconrel.2004.02.002

Cho, C. S., Seo, S. J., Park, I. K., Kim, S. H., Kim, T. H., Hoshiba, T., Harada, I., & Akaike, T. (2006). Galactose-carrying polymers as extracellular matrices for liver tissue engineering. *Biomaterials, 27*(4), 576–585. https://doi.org/10.1016/j.biomaterials.2005.06.008

de Groot, S. C., Sliedregt, K., van Benthem, P. P. G., Rivolta, M. N., & Huisman, M. A. (2020). Building an artificial stem cell niche: Prerequisites for future 3D-Formation of inner ear structures-toward 3D Inner ear biotechnology. *Anatomical Record (Hoboken, N.J.: 2007), 303*(3), 408–426. https://doi.org/10.1002/ar.24067

Di Stefano, A. B., Leto Barone, A. A., Giammona, A., Apuzzo, T., Moschella, P., Di Franco, S., Giunta, G., Carmisciano, M., Eleuteri, C., Todaro, M., Dieli, F., Cordova, A., Stassi, G., & Moschella, F. (2016). Identification and expansion of adipose stem cells with enhanced bone regeneration properties. *Journal of Regenerative Medicine, 05*(01). https://doi.org/10.4172/2325-9620.1000124

Di Stefano, A. B., Montesano, L., Belmonte, B., Gulino, A., Gagliardo, C., Florena, A. M., Bilello, G., Moschella, F., Cordova, A., Leto Barone, A. A., & Toia, F. (2021). Human spheroids from adipose-derived stem cells induce calvarial bone production in a xenogeneic rabbit model. *Annals of Plastic Surgery, 86*(6), 714–720. https://doi.org/10.1097/SAP.0000000000002579

Dispenza, C., Todaro, S., Sabatino, M. A., Chillura Martino, D., Martorana, V., San Biagio, P. L., Maffei, P., & Bulone, D (2020). Multi-scale structural analysis of xyloglucan colloidal dispersions and hydro-alcoholic gels. *Cellulose, 27*(6), 3025–3035. https://doi.org/10.1007/s10570-020-03004-0

El-Fawal, G. F., Yassin, A. M., & El-Deeb, N. M. (2017). The novelty in fabrication of poly vinyl Alcohol/κ-Carrageenan hydrogel with lactobacillus bulgaricus extract as anti-inflammatory wound dressing agent. *AAPS PharmSciTech, 18*(5), 1605–1616. https://doi.org/10.1208/s12249-016-0628-6

Fitzpatrick, L. E., & McDevitt, T. C. (2015). Cell-derived matrices for tissue engineering and regenerative medicine applications. *Biomaterials Science, 3*(1), 12–24. https://doi.org/10.1039/C4BM00246F

Ho, S. S., Murphy, K. C., Binder, B. Y. K., Vissers, C. B., & Leach, J. K. (2016). Increased survival and function of mesenchymal stem cell spheroids entrapped in instructive alginate hydrogels. *Stem Cells Translational Medicine, 5*(6), 773–781. https://doi.org/10.5966/sctm.2015-0211

Hoshiba, T., Lu, H., Kawazoe, N., & Chen, G. (2010). Decellularized matrices for tissue engineering. *Expert Opinion on Biological Therapy, 10*(12), 1717–1728. https://doi.org/10.1517/14712598.2010.534079

Janmey, P. A., Fletcher, D. A., & Reinhart-King, C. A. (2020). Stiffness sensing by cells. *Physiological Reviews, 100*(2), 695–724. https://doi.org/10.1152/physrev.00013.2019

Klíma, J., Lacina, L., Dvořánková, B., Herrmann, D., Carnwath, J. W., Niemann, H., Kaltner, H., André, S., Motlík, J., Gabius, H.-J., & Smetana, K. (2009). Differential regulation of galectin expression/reactivity during wound healing in porcine skin and in cultures of epidermal cells with functional impact on migration. *Physiological Research, 58*(6), 873–884. https://doi.org/10.33549/physiolres.931624

Li, Y. J., Chung, E. H., Rodriguez, R. T., Firpo, M. T., & Healy, K. E. (2006). Hydrogels as artificial matrices for human embryonic stem cell self-renewal. *Journal of Biomedical Materials Research Part A, 79A*(1), 1–5. https://doi.org/10.1002/jbm.a.30732

Liang, Y., Walczak, P., & Bulte, J. W. M. (2013). The survival of engrafted neural stem cells within hyaluronic acid hydrogels. *Biomaterials, 34*(22), 5521–5529. https://doi.org/10.1016/j.biomaterials.2013.03.095

Liu, J. F., Chen, Y. M., Yang, J. J., Kurokawa, T., Kakugo, A., Yamamoto, K., & Gong, J. P. (2011). Dynamic behavior and spontaneous differentiation of mouse embryoid bodies on hydrogel substrates of different surface charge and chemical structures. *Tissue Engineering Part A, 17*(17–18), 2343–2357. https://doi.org/10.1089/ten.tea.2011.0034

Liu, J., Willför, S., & Xu, C. (2015). A review of bioactive plant polysaccharides: Biological activities, functionalization, and biomedical applications. *Bioactive Carbohydrates and Dietary Fibre, 5*(1), 31–61. https://doi.org/10.1016/j.bcdf.2014.12.001

Maeno, S., Niki, Y., Matsumoto, H., Morioka, H., Yatabe, T., Funayama, A., Toyama, Y., Taguchi, T., & Tanaka, J. (2005). The effect of calcium ion concentration on osteoblast viability, proliferation and differentiation in monolayer and 3D culture. *Biomaterials, 26*(23), 4847–4855. https://doi.org/10.1016/j.biomaterials.2005.01.006

Mangione, M. R., Giacomazza, D., Bulone, D., Martorana, V., & San Biagio, P. L. (2003). Thermoreversible gelation of κ-Carrageenan: Relation between conformational transition and aggregation. *Biophysical Chemistry, 104*(1), 95–105. https://doi.org/10.1016/S0301-4622(02)00341-1

Muscolino, E., Costa, M. A., Sabatino, M. A., Alessi, S., Bulone, D., San Biagio, P. L., Passantino, R., Giacomazza, D., & Dispenza, C. (2022). Recombinant mussel protein Pvfp5β enhances cell adhesion of poly(vinyl alcohol)/k-carrageenan hydrogel scaffolds. *International Journal of Biological Macromolecules, 211*, 639–652. https://doi.org/10.1016/j.ijbiomac.2022.05.068

Muscolino, E., Di Stefano, A. B., Trapani, M., Sabatino, M. A., Giacomazza, D., Alessi, S., Cammarata, E., Moschella, F., Cordova, A., Toia, F., & Dispenza, C. (2022). κ-Carrageenan and PVA blends as bioinks to 3D print scaffolds for cartilage reconstruction. *International Journal of Biological Macromolecules, 222*, 1861–1875. https://doi.org/10.1016/j.ijbiomac.2022.09.275

Muscolino, E., Di Stefano, A. B., Trapani, M., Sabatino, M. A., Giacomazza, D., Moschella, F., Cordova, A., Toia, F., & Dispenza, C. (2021). Injectable xyloglucan hydrogels incorporating spheroids of adipose stem cells for bone and cartilage regeneration. *Materials Science and Engineering: C, 131*, Article 112545. https://doi.org/10.1016/j.msec.2021.112545

Muscolino, E., Sabatino, M. A., Jonsson, M., & Dispenza, C. (2023). The role of water in radiation-induced fragmentation of cellulosic backbone polysaccharides. *Cellulose*. https://doi.org/10.1007/s10570-023-05660-4

Nayyer, L., Patel, K. H., Esmaeili, A., Rippel, R. A., Birchall, M., O'Toole, G., Butler, P. E., & Seifalian, A. M. (2012). Tissue engineering: Revolution and challenge in auricular cartilage reconstruction. *Plastic and Reconstructive Surgery, 129*(5), 1123–1137. https://doi.org/10.1097/PRS.0b013e31824a2c1c

Necas, J., & Bartosikova, L. (2013). Carrageenan: A review. *Veterinární Medicína, 58*(4), 187–205. https://doi.org/10.17221/6758-VETMED

Panjwani, N. (2014). Role of galectins in re-epithelialization of wounds. *Annals of Translational Medicine, 2*(9), 89. https://doi.org/10.3978/j.issn.2305-5839.2014.09.09

Petzold, J., & Gentleman, E. (2021). Intrinsic mechanical cues and their impact on stem cells and embryogenesis. *Frontiers in Cell and Developmental Biology, 9*, Article 761871. https://doi.org/10.3389/fcell.2021.761871

Picone, P., Muscolino, E., Girgenti, A., Testa, M., Giacomazza, D., Dispenza, C., & Nuzzo, D. (2024). Mitochondria embedded in degalactosylated xyloglucan hydrogels to improve mitochondrial transplantation. *Carbohydrate Polymer Technologies and Applications, 8*, Article 100543. https://doi.org/10.1016/j.carpta.2024.100543

Reilly, G. C., & Engler, A. J. (2010). Intrinsic extracellular matrix properties regulate stem cell differentiation. *Journal of Biomechanics, 43*(1), 55–62. https://doi.org/10.1016/j.jbiomech.2009.09.009

Rinaudo, M. (1993). Gelation of polysaccharides. *Journal of Intelligent Material Systems and Structures, 4*(2), 210–215. https://doi.org/10.1177/1045389×9300400210

Shih, Y.-R. V., Tseng, K.-F., Lai, H.-Y., Lin, C.-H., & Lee, O. K. (2011). Matrix stiffness regulation of integrin-mediated mechanotransduction during osteogenic differentiation of human mesenchymal stem cells. *Journal of Bone and Mineral Research, 26*(4), 730–738. https://doi.org/10.1002/jbmr.278

Shirakawa, M., Yamatoya, K., & Nishinari, K. (1998). Tailoring of xyloglucan properties using an enzyme. *Food Hydrocolloids, 12*(1), 25–28. https://doi.org/10.1016/S0268-005X(98)00052-6

Shrestha, K. R., & Yoo, S. Y. (2019). Phage-based artificial niche: The recent progress and future opportunities in stem cell therapy. *Stem Cells International, 2019*, Article 4038560. https://doi.org/10.1155/2019/4038560

Stephens, M. B., Beutler, A. I., & O'Connor, F. G. (2008). Musculoskeletal injections: A review of the evidence. *American Family Physician, 78*(8), 971–976.

Stoddart, M. J., Grad, S., Eglin, D., & Alini, M. (2009). Cells and biomaterials in cartilage tissue engineering. *Regenerative Medicine, 4*(1), 81–98. https://doi.org/10.2217/17460751.4.1.81

Todaro, S., Dispenza, C., Sabatino, M. A., Ortore, M. G., Passantino, R., San Biagio, P. L., & Bulone, D. (2015). Temperature-induced self-assembly of degalactosylated xyloglucan at low concentration. *Journal of Polymer Science Part B: Polymer Physics, 53*(24), 1727–1735. https://doi.org/10.1002/polb.23895

Todaro, S., Sabatino, M. A., Mangione, M. R., Picone, P., Di Giacinto, M. L., Bulone, D., & Dispenza, C. (2016). Temporal control of xyloglucan self-assembly into layered structures by radiation-induced degradation. *Carbohydrate Polymers, 152*, 382–390. https://doi.org/10.1016/j.carbpol.2016.07.005

Toia, F., Di Stefano, A. B., Muscolino, E., Sabatino, M. A., Giacomazza, D., Moschella, F., Cordova, A., & Dispenza, C. (2020). In-situ gelling xyloglucan formulations as 3D artificial niche for adipose stem cell spheroids. *International Journal of Biological Macromolecules, 165*, 2886–2899. https://doi.org/10.1016/j.ijbiomac.2020.10.158

Vo, A., Doumit, M., & Rockwell, G. (2016). The biomechanics and optimization of the needle-syringe system for injecting triamcinolone acetonide into keloids. *Journal of Medical Engineering, 2016*, 1–8. https://doi.org/10.1155/2016/5162394

Watt, R. P., Khatri, H., & Dibble, A. R. G. (2019). Injectability as a function of viscosity and dosing materials for subcutaneous administration. *International Journal of Pharmaceutics, 554*, 376–386. https://doi.org/10.1016/j.ijpharm.2018.11.012

Witkowska-Zimny, M., Walenko, K., Wrobel, E., Mrowka, P., Mikulska, A., & Przybylski, J. (2013). Effect of substrate stiffness on the osteogenic differentiation of bone marrow stem cells and bone-derived cells. *Cell Biology International, 37*(6), 608–616. https://doi.org/10.1002/cbin.10078

Wu, D. T., Diba, M., Yang, S., Freedman, B. R., Elosegui-Artola, A., & Mooney, D. J. (2023). Hydrogel viscoelasticity modulates migration and fusion of mesenchymal stem cell spheroids. *Bioengineering & Translational Medicine, 8*(3), e10464. https://doi.org/10.1002/btm2.10464

Yin, C. (2003). Adhesion contact dynamics of HepG2 cells on galactose-immobilized substrates. *Biomaterials, 24*(5), 837–850. https://doi.org/10.1016/S0142-9612(02)00416-7

Zhang, Y., Ye, L., Cui, M., Yang, B., Li, J., Sun, H., & Yao, F. (2015). Physically crosslinked poly(vinyl alcohol)–carrageenan composite hydrogels: Pore structure stability and cell adhesive ability. *RSC Advances, 5*(95), 78180–78191. https://doi.org/10.1039/C5RA11331H

Zhu, J., & Marchant, R. E. (2011). Design properties of hydrogel tissue-engineering scaffolds. *Expert Review of Medical Devices, 8*(5), 607–626. https://doi.org/10.1586/erd.11.27

Žigon-Branc, S., Markovic, M., Van Hoorick, J., Van Vlierberghe, S., Dubruel, P., Zerobin, E., Baudis, S., & Ovsianikov, A. (2019). Impact of hydrogel stiffness on differentiation of human adipose-derived stem cell microspheroids. *Tissue Engineering Part A, 25*(19–20), 1369–1380. https://doi.org/10.1089/ten.tea.2018.0237